Journal of Organometallic Chemistry, 473 (1994) 187–193

Reactions of sterically congested secondary silanes with iron carbonyls. Formation of μ-silylene complexes $Fe_2(CO)_8(\mu\text{-}SiR_2)$ (R = mesityl and $O(2,6\text{-}^iPr_2C_6H_3)$)

Hiromi Tobita, Isao Shinagawa, Setsuko Ohnuki, Machiko Abe, Hiroshi Izumi and Hiroshi Ogino

Department of Chemistry, Faculty of Science, Tohoku University, Aoba-ku, Sendai 980 (Japan)

(Received December 8, 1993; in revised form January 19, 1994)

Abstract

Reaction of dimesitylsilane with enneacarbonyldiiron in hot hexane yielded octacarbonyl(μ-dimesitylsilylene)diiron as thermally stable yellow crystals, for which the average bond lengths determined by X-ray crystallography are Fe–Fe 2.721(2) and Fe–Si 2.404(2) Å, and the ^{29}Si NMR chemical shift of the bridging silylene is 145.1 ppm. Similarly, the reaction of bis(2,6-diisopropylphenoxy)silane with dodecacarbonyltriiron in refluxing toluene afforded octacarbonyl{μ-bis(2,6-diisopropylphenoxy)silylene}diiron, whereas a similar treatment of the slightly bulkier bis(2,6-di-tert-butylphenoxy)silane with enneacarbonyldiiron or dodecacarbonyltriiron did not give the corresponding μ-silylene complex.

Key words: Iron; Silicon; Secondary silanes; Carbonyl; μ-Silylene; X-ray diffraction

1. Introduction

A dinuclear complex containing a metal–metal bond singly bridged by a silylene ligand is the simplest model for μ-silylene species bound to a metal surface. Nevertheless, hitherto, there has been only one reported example of this type of complex, *i.e.* $Fe_2(CO)_8(\mu\text{-}SiMe_2)$ [1]. This dark-red complex was prepared in low yield (8%) from Me_2SiHCl and $Fe_2(CO)_9$ in the presence of amine, but was reported to be flammable in air and stable only at low temperature under an inert atmosphere. We recently found that the reactions of sterically congested secondary silanes with iron carbonyls give thermally stable $Fe_2(CO)_8(\mu$-silylene) in fair yields. We report here the syntheses and properties of the $Fe_2(CO)_8(\mu$-silylene) complexes and the first X-ray crystal structure of a silylene-bridged diiron octacarbonyl complex.

Correspondence to: Dr. H. Tobita or Dr. H. Ogino.

2. Experimental details

2.1. General procedure

Standard Schlenk techniques were employed in handling organosilyl and organoiron compounds, and all manipulations were performed under a nitrogen atmosphere. Reagent-grade hexane, pentane, toluene and tetrahydrofuran were distilled under a nitrogen atmosphere from sodium-benzophenone ketyl immediately before use. Mes_2SiH_2 (**1a**) (Mes = 2,4,6-trimethylphenyl) [2] was prepared by the reduction of Mes_2SiCl_2 [3] with $LiAlH_4$ in ether. $Fe_2(CO)_9$ [4] and $Fe_3(CO)_{12}$ [5] were prepared according to published procedures. Other chemicals were purchased from Wako Pure Chemical Industries, Ltd. and used without further purification.

^{1}H, ^{13}C and ^{29}Si NMR spectra were recorded on Jeol FX-90Q and Varian XL-200 NMR spectrometers. IR spectra were obtained on Jasco IR-810 and Bruker IFS66v spectrophotometers. Mass spectra were taken on Hitachi M-52 and Jeol JMS-HX110 mass spectrometers, and high resolution mass spectra on a Jeol JMS-

0022-328X/94/$7.00
SSDI 0022-328X(94)24481-W

HX110 mass spectrometer. Temperature-dependent ^1H and ^{13}C NMR spectra were recorded on the Jeol FX-90Q machine using CD_2Cl_2 as a solvent.

2.2. Preparation of bis(2,6-diisopropylphenoxy)silane (1b)

2,6-Diisopropylphenol (10.0 g, 56.1 mmol) was dissolved in THF (100 ml) and NaH (60% in mineral oil, 2.60 g, 65 mmol) was added in portions to the solution with stirring. The reaction was exothermic. Dichlorosilane (2.00 ml, 2.84 g, 28.1 mmol) was condensed in another flask cooled to −38°C in a CH_3CN/liq. N_2 bath and THF (50 ml) was added. The former solution containing 2,6-$^iPr_2C_6H_3ONa$ was added to the cold solution of dichlorosilane *via* a cannula, and the mixture was stirred at −38°C for 40 min. The mixture was then stirred overnight at room temperature and finally refluxed for 2 h. The salt (NaCl) was removed by centrifugation and the supernatant liquid was evaporated under reduced pressure. Molecular distillation of the residue (120°C/0.05 Torr) followed by distillation (125–138°C/0.12 Torr) gave $\{(2,6\text{-}^iPr_2C_6H_3)O\}_2SiH_2$ (**1b**) (6.07 g, 15.8 mmol, 56%) as a colorless liquid. ^1H NMR (200 MHz, C_6D_6): δ 1.19 (24H, d, $J = 6.8$ Hz, $CHMe_2$); 3.43 (4H, sep, $J = 6.8$ Hz, $CHMe_2$); 5.18 (2H, s, Si–H); 6.74–7.03 (6H, m, Ar–H). ^{13}C NMR (50.3 MHz, C_6D_6): δ 23.6 ($CHMe_2$); 27.7 ($CHMe_2$), 123.9, 124.2, 139.1, 148.7 (ring-C). ^{29}Si NMR (17.8 MHz, C_6D_6): δ −37.3. IR (neat, NaCl): ν(Si–H) 2200 cm^{-1}. MS (EI): *m/z* 384 (26, M^+), 383 (59, $M^+ - 1$), 207 (11, $M^+ - O(^iPr_2C_6H_3)$), 206 (31, $M^+ - HO(^iPr_2C_6H_3)$), 178 (95, $HO(^iPr_2C_6H_3)^+$), 163 (100, $HO(^iPr_2C_6H_3)^+ - Me$).

2.3. Preparation of bis(2,6-di-tert-butylphenoxy)silane (1c)

In a manner similar to the preparation of **1b**, a solution of 2,6-$^tBu_2C_6H_3ONa$ prepared from 2,6-di-tert-butylphenol (10.2 g, 49.3 mmol) and NaH (60%, 2.48 g, 62.0 mmol) was added to a cold solution of dichlorosilane (4.00 ml, 56.2 mmol). After a similar workup, recrystallization from hexane afforded $\{(2,6\text{-}^tBu_2C_6H_3)O\}_2SiH_2$ (**1b**) (6.15 g, 13.9 mmol, 57%) as colorless crystals. ^1H NMR (90 MHz, C_6D_6): δ 1.51 (36H, s, CMe_3); 5.27 (2H, s, Si–H); 6.84–7.35 (6H, m, Ar–H). ^{13}C NMR (22.5 MHz, C_6D_6): δ 31.9 (CMe_3); 35.3 (CMe_3), 122.7, 126.5, 141.9, 152.0 (ring-C). ^{29}Si NMR (17.8 MHz, C_6D_6): δ −37.0. IR (KBr pellet): ν(Si–H) 2200 cm^{-1}. MS (EI): *m/z* 440 (24, M^+), 233 (20, $^tBu_2C_6H_3OSi^+$), 57 (100, $C_4H_9^+$). Anal. Found: C, 76.10; H, 9.89. $C_{28}H_{44}O_2Si$ calcd.: C, 76.31; H, 10.06%.

2.4. Reaction of dimesitylsilane (1a) with $Fe_2(CO)_9$

A mixture of dimesitylsilane (1.03 g, 3.84 mmol) and $Fe_2(CO)_9$ (9.02 g, 24.8 mmol) was heated in hexane at 72°C for 39 h. At this point, the silica gel TLC (hexane/benzene 10:1) showed the spots of $Fe_3(CO)_{12}$ and the remaining dimesitylsilane, so that $Fe_2(CO)_9$ (1.00 g, 2.75 mmol) was added to the reaction mixture and the mixture was heated for an additional 3 h. After cooling to room temperature, the mixture was passed through a Florisil short column and the column was washed with CH_2Cl_2. Removal of the solvent *in vacuo* from the eluate afforded a green residue. Dimesitylsilane and $Fe_3(CO)_{12}$ were removed from this residue by sublimation under a high vacuum (48°C/5.5×10^{-5} Torr). Recrystallization of the remaining yellow-orange powder from a mixed solvent of hexane/benzene (5:1) provided $Fe_2(CO)_8(\mu\text{-}SiMes_2)$ (**2a**) (960 mg, 1.59 mmol, 42%) as orange crystals. ^1H NMR (90 MHz, C_6D_6): δ 2.00 (6H, s, *p*-Me); 2.70 (12H, s, *o*-Me); 6.64 (4H, s, Ar–H). ^{13}C NMR (50 MHz, C_6D_6): δ 20.8 (*p*-Me); 24.8 (*o*-Me); 130.1, 139.1, 141.9 (ring-C); 206.9, 211.8 (CO). ^{29}Si NMR (17.8 MHz, C_6D_6): δ 145.1. IR (KBr pellet): ν(CO) 2090, 2044, 2024, 2016, 2000, 1982 cm^{-1}. MS (EI): *m/z* 602 (4.7, M^+), 574 (1.0, $M^+ - CO$), 546 (3.5, $M^+ - 2CO$), 518 (10, $M^+ - 3CO$), 490 (8.2, $M^+ - 4CO$), 483 (12, $M^+ - Mes$), 462 (23, $M^+ - 5CO$), 434 (8.2, $M^+ - 6CO$), 406 (90, $M^+ - 7CO$), 378 (18, $M^+ - 8CO$), 350 (100, $M^+ - 7CO - Fe$), 322 (29, $M^+ - 8CO - Fe$). Exact mass calculated for $C_{26}H_{22}O_8Fe_2Si$: 601.9783. Found: 601.9780.

2.5. Reaction of bis(2,6-diisopropylphenoxy)silane (1b) with $Fe_3(CO)_{12}$

A solution of **1b** (325 mg, 0.845 mmol) and $Fe_3(CO)_{12}$ (340 mg, 0.675 mmol) in toluene (20 ml) was refluxed with stirring for 16 h. After removal of the solvent *in vacuo*, the residue was dissolved in pentane and the solution was cooled down to −78°C to give $Fe_2(CO)_8[\mu\text{-}Si\{O(2,6\text{-}^iPr_2C_6H_3)\}_2]$ (**2b**) (257 mg, 0.358 mmol, 42%) as orange crystals. ^1H NMR (90 MHz, CD_2Cl_2, r.t.): δ 1.08 (24H, br d, $J = 6.4$ Hz, $CHMe_2$); 3.28 (4H, sep, $J = 6.4$ Hz, $CHMe_2$); 6.92–6.99 (6H, m, Ar–H). ^{13}C NMR (50 MHz, CD_2Cl_2, r.t.): δ 23.0, 23.6 (br, $CHMe_2$); 28.5 ($CHMe_2$), 123.6, 134.2, 138.4, 149.8 (ring-C), 209.8 (CO). ^{29}Si NMR (17.8 MHz, C_6D_6, tris(acetylacetonato)chromium(III) as a relaxation reagent): δ 88.4. IR (KBr pellet): ν(CO) 2115, 2060, 2040, 2025, 1993 cm^{-1}. MS (EI): *m/z* 718 (52, M^+), 634 (16, $M^+ - 3CO$), 606 (64, $M^+ - 4CO$), 578 (69, $M^+ - 5CO$), 522 (69, $M^+ - 7CO$), 494 (5.5, $M^+ - 8CO$), 438 (100, $M^+ - 8CO - Fe$). Exact mass calculated for $C_{32}H_{34}O_{10}Fe_2Si$: 718.0621. Found: 718.0645.

2.6. Reaction of bis(2,6-di-tert-butylphenoxy)silane (1c) with $Fe_3(CO)_{12}$ or $Fe_2(CO)_9$

A mixture of **1c** (452 mg, 1.03 mmol) and $Fe_3(CO)_{12}$ (392 mg, 0.778 mmol) in toluene (20 ml) was refluxed

TABLE 1. Crystal data for $Fe_2(CO)_8(\mu\text{-}SiMes_2)$ (**2a**)

Formula	$C_{26}H_{22}Fe_2O_8Si$
F.W.	602.2
Crystal system	Triclinic
Space group	$P\bar{1}$
a (Å)	14.342(3)
b (Å)	17.508(4)
c (Å)	12.617(2)
α (°)	106.54(2)
β (°)	90.77(2)
γ (°)	112.52(2)
V (Å^3)	2778.4(9)
Z	4
d_{calcd} (g cm^{-3})	1.45
μ (Mo-Kα) (cm^{-1})	11.6
Crystal size (mm)	0.38×0.3×0.25
2θ range (°)	3–50
Scan mode	ω–2θ
ω-scan width (°)	1.0
No. of unique data	9591
No. of data used with $\|F_o\| > 3\sigma(F_o)$	5493
R [a]	0.062
R_w [b]	0.078

[a] $R = \Sigma \| F_o \| - \| F_c \| / \Sigma | F_o |$. [b] $R_w = [\Sigma w(| F_o | - | F_c |)^2 / \Sigma w | F_o |^2]^{1/2}$; $w = [\sigma^2(|F_o|) + aF_o^2]^{-1}$, where $a = 0.0015$.

and the reaction was monitored by silica gel TLC (toluene/hexane 1:10). After 23 h, only the spot of **1c** was left on the TLC. After removal of the solvent, the residue was extracted with pentane and the extract was evaporated to dryness. Ninety percent of **1c** was recovered. In a similar manner, after refluxing the mixture of **1c** (439 mg, 0.996 mmol) and $Fe_2(CO)_9$ (747 mg, 2.05 mmol) in hexane (15 ml) for 52 h, 100% of **1c** was recovered.

2.7. X-Ray crystal structure analysis of $Fe_2(CO)_8(\mu\text{-}SiMes_2)$ (2a)

Diffraction measurements were made on a Rigaku AFC-6A four-circle diffractometer with graphite-monochromated Mo-Kα radiation ($\lambda = 0.71073$ Å). Crystal data are listed in Table 1. The structure was solved by the heavy-atom method and refined by the block-diagonal least-squares method using individual anisotropic thermal parameters for the non-hydrogen atoms and isotropic thermal parameters for hydrogen atoms. The positions of 8 *meta*-hydrogens of the mesityl groups in two independent molecules were calculated and fixed. The final atomic parameters and temperature factors of non-hydrogen atoms are listed in Table 2.

The calculations were performed on a Nippon Electric Co. ACOS-2000 computer system at the Computer Center of Tohoku University using the Universal Crystallographic Computation Program System UNICS III [6].

Further details of the crystal structure investigation are available on request from the Director of the Cambridge Crystallographic Data Centre, University Chemical Laboratory, Lensfield Road, Cambridge CB2 1EW (UK), on quoting the full journal citation.

3. Results and discussion

The sterically congested secondary silanes, $\{(2,6\text{-}^iPr_2C_6H_3)O\}_2SiH_2$ (**1b**) and $\{(2,6\text{-}^tBu_2C_6H_3)O\}_2SiH_2$ (**1c**), were prepared by the reaction of the corresponding sodium phenoxides with dichlorosilane (eqn. (1)). To our knowledge, these are the first examples of diphenoxysilane derivatives except for the parent diphenoxysilane [7]. Dichlorosilane has the following advantages over tri- or tetrachlorosilanes as starting materials for the preparation of diphenoxysilanes: (1) dichlorosilane is less bulky than trichlorosilane or tetrachlorosilane and thus more reactive towards bulky nucleophiles, and (2) diphenoxysilanes can be prepared in one step without any reduction process which may break the Si–phenoxy bonds [8]. These diphenoxysilanes were fully characterized by spectroscopic and elemental analysis.

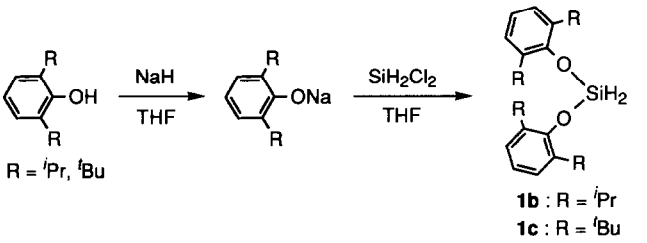

(1)

Reaction of Mes_2SiH_2 (**1a**) with excess $Fe_2(CO)_9$ in refluxing hexane afforded the dimesitylsilylene-bridged diiron complex $Fe_2(CO)_8(\mu\text{-}SiMes_2)$ (**2a**) as orange crystals in 42% yield (eqn. (2)). For the reaction of the bulkier **1b** with iron carbonyl, a higher reaction temperature was necessary, and the best yield of $Fe_2(CO)_8[\mu\text{-}Si\{O(2,6\text{-}^iPr_2C_6H_3)\}_2]$ (**2b**) (42%) was obtained upon refluxing a toluene solution of **1b** and $Fe_3(CO)_{12}$ (eqn. (3)). Crystals of **1a** and **1b** are thermally stable at room temperature and are also fairly stable in air. Interestingly, refluxing a toluene solution of $Fe_3(CO)_{12}$ and **1c**, which is only slightly bulkier than **1b**, did not give the corresponding μ-silylene complex $Fe_2(CO)_8[\mu\text{-}Si\{O(2,6\text{-}^tBu_2C_6H_3)\}_2]$ and 90% of **1c** was recovered. Thus, moderate steric congestion of secondary silane seems to be important for the formation

TABLE 2. Final atomic parameters and temperature factors of the non-hydrogen atoms of $Fe_2(CO)_8(\mu\text{-}SiMes_2)$ (**2a**) [a]

Atom	x	y	z	B_{eq}
Fe(11)	449.8(7)	956.3(6)	2973.4(8)	4.4
Fe(12)	638.1(7)	2600.2(6)	4087.8(8)	4.1
Si(1)	1624(1)	2240(1)	2642(1)	3.2
O(101)	−573(4)	615(4)	765(5)	8.4
O(102)	−1507(5)	106(5)	3750(7)	11.1
O(103)	1000(4)	−511(3)	2004(5)	7.6
O(104)	1657(7)	1294(5)	5073(5)	11.2
O(105)	2575(4)	3337(4)	5566(4)	7.2
O(106)	809(6)	4352(4)	4366(6)	10.1
O(107)	−1302(4)	1890(5)	2620(6)	9.3
O(108)	−528(4)	2179(4)	5898(5)	8.0
C(101)	−167(5)	786(5)	1610(6)	5.6
C(102)	−743(7)	435(5)	3451(8)	7.2
C(103)	802(6)	65(5)	2371(7)	5.6
C(104)	1209(7)	1212(5)	4270(7)	6.8
C(105)	1856(5)	3037(5)	4966(6)	4.9
C(106)	751(7)	3668(5)	4251(7)	6.7
C(107)	−520(6)	2148(5)	3153(7)	6.0
C(108)	−81(6)	2337(5)	5205(6)	5.5
C(111)	1475(4)	2242(4)	1124(5)	3.5
C(112)	1915(5)	1753(4)	366(5)	4.0
C(113)	1876(5)	1739(5)	−740(6)	5.0
C(114)	1418(5)	2179(5)	−1155(6)	5.1
C(115)	979(5)	2648(4)	−423(6)	4.6
C(116)	984(5)	2683(4)	710(5)	3.9
C(117)	2442(5)	1231(5)	691(6)	4.7
C(118)	1412(7)	2156(6)	−2379(6)	7.5
C(119)	425(6)	3195(5)	1387(7)	6.0
C(121)	3085(4)	2804(4)	3087(5)	3.3
C(122)	3712(5)	2430(4)	3359(5)	3.9
C(123)	4769(5)	2913(5)	3633(6)	4.7
C(124)	5216(5)	3784(5)	3689(6)	5.0
C(125)	4601(5)	4144(4)	3432(6)	4.8
C(126)	3550(5)	3687(4)	3133(5)	4.1
C(127)	3361(6)	1483(5)	3343(8)	6.2
C(128)	6386(6)	4286(6)	3990(8)	7.8
C(129)	2957(6)	4178(5)	2823(7)	5.6
Fe(21)	4662.3(7)	9057.7(6)	1768.8(9)	4.6
Fe(22)	3227.6(7)	8293.5(6)	2956.3(8)	4.0
Si(2)	3811(1)	7515(1)	1396(2)	3.4
O(201)	6446(4)	8807(4)	2531(6)	8.0
O(202)	5604(6)	10894(4)	3169(6)	10.2
O(203)	5468(4)	9264(4)	−296(5)	7.6
O(204)	2870(4)	9284(4)	1029(6)	8.1
O(205)	1288(4)	7481(4)	1456(5)	7.1
O(206)	2343(5)	7104(5)	4248(6)	9.6
O(207)	5132(4)	9084(4)	4490(5)	7.9
O(208)	2657(4)	9737(3)	4140(5)	7.4
C(201)	5733(5)	8876(4)	2244(7)	5.3
C(202)	5224(7)	10187(5)	2670(8)	6.9
C(203)	5157(6)	9163(5)	510(7)	5.7
C(204)	3522(6)	9153(5)	1349(7)	6.0
C(205)	2050(5)	7792(5)	1978(6)	4.8
C(206)	2682(6)	7547(5)	3718(7)	5.8
C(207)	4437(6)	8789(5)	3831(6)	5.6
C(208)	2896(5)	9202(5)	3684(6)	5.1
C(211)	4712(4)	6937(4)	1410(5)	3.4
C(212)	5157(5)	6739(4)	431(6)	4.0
C(213)	5782(5)	6294(4)	341(6)	4.8
C(214)	6016(5)	6035(4)	1196(7)	5.2
C(215)	5625(5)	6249(4)	2169(6)	4.6
C(216)	4972(5)	6692(4)	2310(6)	4.3
C(217)	4953(6)	6982(5)	−600(6)	5.3
C(218)	6707(6)	5541(5)	1095(9)	7.3
C(219)	4607(7)	6891(6)	3447(6)	6.4
C(221)	2730(5)	6684(4)	195(6)	3.9
C(222)	2486(5)	6794(5)	−817(6)	4.8
C(223)	1708(6)	6103(5)	−1616(6)	5.7
C(224)	1162(6)	5320(5)	−1451(7)	6.0
C(225)	1384(5)	5223(4)	−463(7)	5.4
C(226)	2157(5)	5882(4)	375(6)	4.5
C(227)	2999(7)	7616(6)	−1141(7)	7.4
C(228)	333(8)	4558(7)	−2387(9)	10.1
C(229)	2338(6)	5671(5)	1430(7)	5.9

[a] Positional parameters are multiplied by 10^4. Thermal parameters are given by the equivalent temperature factors ($Å^2$).

and stabilization of the singly silylene-bridged diiron complex.

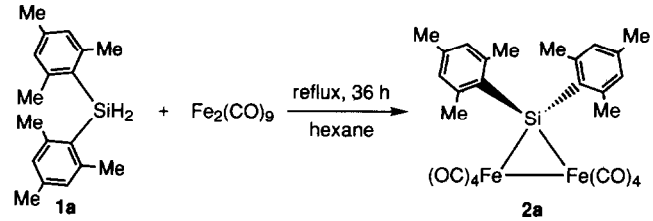

(2)

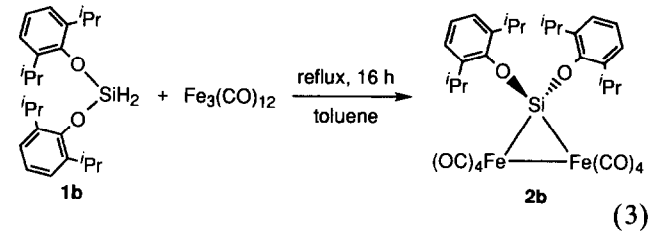

(3)

Each of the mass spectra of **2a** and **2b** exhibits the molecular ion peak and peaks corresponding to the successive loss of eight COs. The IR spectra of **2a** and **2b** show six and five CO-stretching bands, respectively, in the terminal CO region, corresponding to the seven modes $[3A_1 + B_1 + 3B_2]$ predicted for local C_{2v} symmetry. These data as well as the ^1H and ^{13}C NMR spectra support the structures of **2a** and **2b**. In the ^{13}C NMR spectrum, **2a** and **2b** exhibit two and one carbonyl signals, respectively. Therefore, the carbonyl groups in **2a** and **2b** are partly or fully exchanging on the NMR timescale.

The signals of the ^{29}Si NMR spectra of **2a** and **2b** appear at δ 145.1 and 88.4 ppm, respectively. Their low field shifts are smaller than that of the dimethylsilylene-bridged derivative $Fe_2(CO)_8(\mu\text{-}SiMe_2)$ (**3**) (δ 173.0 ppm) [1]. This can be explained by the paramagnetic shielding effect of the substituents on silicon, especially

in the case of **2b** in which the electronegative oxygens are bonded to the silicon atom [9]. It should be noted that these complexes tend to exhibit signals at higher field than other types of μ-silylene complexes which possess two cyclopentadienyl ligands and a μ-CO ligand simultaneously such as $(\mu\text{-}C_5H_5)_2Fe_2(CO)_2(\mu\text{-}CO)(\mu\text{-}SiH^tBu)$ (**4**) (δ 254.4 ppm) [10,11].

The X-ray crystal structure analysis of **2a** was performed for a crystal obtained from a hexane/benzene (5:1) solution. This crystal contains two independent molecules 1 and 2, but there is no essential structural difference between them. The structures of molecule 1 viewed from two different directions are shown in Fig. 1 and the selected bond distances and angles are listed in Tables 3 and 4. The complex consists of a $SiFe_2$ triangle in which the silicon atom bears two mesityl groups and each iron atom carries four terminal carbonyl ligands. Although this is the first structural investigation on a diiron complex containing an iron–iron bond bridged only by a silylene group, the crystal structures of closely related complexes, **4** and $Si[Fe_2(CO)_8]_2$ (**5**), have been reported by us [10] and Anema *et al.* [12], respectively. Some main structural features of **2a**, **4** and **5** are summarized in Table 5 for comparison.

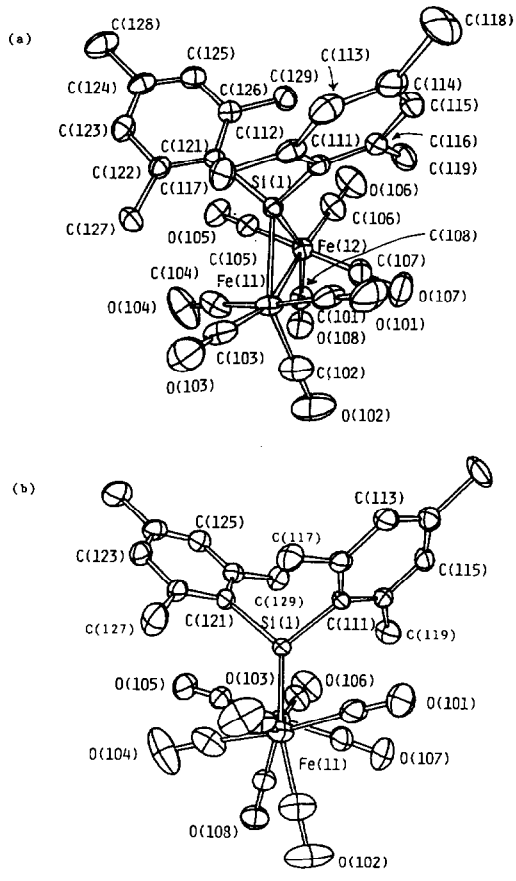

Fig. 1. ORTEP drawings of $Fe_2(CO)_8(\mu\text{-}SiMes_2)$ (**2a**) (molecule 1).

TABLE 3. Selected bond distances (Å) for $Fe_2(CO)_8(\mu\text{-}SiMes_2)$ (**2a**)

	$n=1$	$n=2$
Fe(n1)–Fe(n2)	2.725(2)	2.717(2)
Fe(n1)–Si(n)	2.391(2)	2.397(2)
Fe(n2)–Si(n)	2.413(2)	2.413(2)
Fe(n1)–C(n01)	1.815(10)	1.810(9)
Fe(n1)–C(n02)	1.807(10)	1.823(7)
Fe(n1)–C(n03)	1.792(9)	1.776(11)
Fe(n1)–C(n04)	1.795(11)	1.795(10)
Fe(n2)–C(n05)	1.818(8)	1.827(7)
Fe(n2)–C(n06)	1.764(10)	1.787(10)
Fe(n2)–C(n07)	1.784(9)	1.797(8)
Fe(n2)–C(n08)	1.818(10)	1.833(8)
C(n01)–O(n01)	1.111(12)	1.141(11)
C(n02)–O(n02)	1.152(13)	1.122(9)
C(n03)–O(n03)	1.126(11)	1.149(14)
C(n04)–O(n04)	1.136(15)	1.139(13)
C(n05)–O(n05)	1.119(10)	1.117(9)
C(n06)–O(n06)	1.135(13)	1.141(14)
C(n07)–O(n07)	1.154(11)	1.136(11)
C(n08)–O(n08)	1.128(12)	1.126(11)
Si(n)–C(n11)	1.925(8)	1.924(8)
Si(n)–C(n21)	1.936(6)	1.942(6)

The Fe–Fe bond of **2a** is shorter than that of **5**, but longer than that of **4**. The latter is apparently because the absence of a bridging carbonyl allows the lengthening of the Fe–Fe bond to reduce the severe Fe–Si–Fe angular strain. The Si–Fe bonds of **2a** are longer than those of **4** and **5** and are close to typical Si–Fe single bond distances [13], probably because of the large

TABLE 4. Selected bond angles (°) for $Fe_2(CO)_8(\mu\text{-}SiMes_2)$ (**2a**)

	$n=1$	$n=2$
Fe(n2)–Fe(n1)–Si(n)	55.84(5)	55.89(5)
Fe(n1)–Fe(n2)–Si(n)	55.07(6)	55.32(6)
Fe(n1)–Si(n)–Fe(n2)	69.10(7)	68.79(6)
C(n11)–Si(n)–C(n21)	103.2(3)	103.1(3)
Fe(n1)–C(n01)–O(n01)	174.6(9)	175.8(8)
Fe(n1)–C(n02)–O(n02)	179.4(9)	175.5(7)
Fe(n1)–C(n03)–O(n03)	177.9(8)	177.0(1)
Fe(n1)–C(n04)–O(n04)	173.7(9)	172.0(8)
Fe(n2)–C(n05)–O(n05)	174.9(7)	174.2(7)
Fe(n2)–C(n06)–O(n06)	178.8(9)	176.7(1)
Fe(n2)–C(n07)–O(n07)	174.3(8)	171.4(7)
Fe(n2)–C(n08)–O(n08)	179.5(9)	177.2(8)
C(n01)–Fe(n1)–Fe(n2)–C(n07)	33.08	35.57
C(n02)–Fe(n2)–Fe(n2)–C(n08)	27.50	30.36
C(n03)–Fe(n1)–Fe(n2)–C(n06)	94.57	85.98
C(n04)–Fe(n1)–Fe(n2)–C(n05)	28.46	35.20
Dihedral angle between the (Si(n)–C(n11)–C(n21) plane and the Si(n)–Fe(n1)–Fe(n2) plane	102.73	103.79
Dihedral angle between the two mesityl rings	87.59	95.56

TABLE 5. Structural features of **2a**, **4** and **5** [a]

	Fe–Fe (Å)	Si–Fe (Å)	Fe–Si–Fe (°)	Ref.
$Fe_2(CO)_8(\mu\text{-}SiMes_2)$ (**2a**)	2.721	2.404	68.95	This work
$(\eta\text{-}C_5H_5)_2Fe_2(CO)_2(\mu\text{-}CO)(\mu\text{-}SiH^tBu)$ (**4**)	2.614	2.271	70.28	8
$Si[Fe_2(CO)_8]_2$ (**5**)	2.793	2.347	73.1	10

[a] Average values given.

steric repulsion between bulky mesityl groups on silicon and the carbonyls of the $Fe_2(CO)_8$ moiety. This lengthening of the Si–Fe bonds makes the Fe–Si–Fe angle of **2a** smaller than others.

A characteristic feature of the structure of complex **2a** is the *gauche* conformation of the six CO ligands around the Fe–Fe bond (Fig. 1(b)). The average twist angle of the three pairs of CO ligands from the eclipsed conformation is 29.68° (molecule 1) and 33.71° (molecule 2). Another structural feature is the dihedral angle between the planes containing $SiFe_2$ and SiC_2, *i.e.* 102.73° (molecule 1) and 103.79° (molecule 2), which deviate considerably from a right angle. The origin of these distortions is evidently the adoption by the mesityl groups of a specific dihedral angle between them in order to minimize the steric repulsion between their *ortho*-methyl groups. In fact, the interatomic distances between the carbons of *ortho*-methyl groups are 3.42(2) (C(117) · · · C(127)) and 3.56 (C(119) · · · C(129)) Å, respectively, and are slightly less than the sum of the effective van der Waals radii of methyl groups (4.0 Å). As a result, two methyl groups with C(119) and C(127) are oriented towards the $Fe_2(CO)_8$ moiety and have strong steric interactions with certain carbonyl ligands. Thus, the interatomic distances between oxygen atoms of axial carbonyl ligands on the $SiFe_2$ plane and the carbon atoms of *ortho*-methyls of the mesityl groups are 3.28(1) (O(104) · · · C(127)) and 3.40(1) Å (O(107) · · · C(119)), respectively, and are comparable with the sum of the effective van der Waals radii of an oxygen atom and a methyl group (3.40 Å). Moreover, the four axial carbonyl ligands (containing C(*n*01), C(*n*04), C(*n*05), and C(*n*07)) are bent away at the carbon atoms from the mesityl groups; Fe–C–O = 171.4–175.8°. These steric interactions result in the twisting of **2a**.

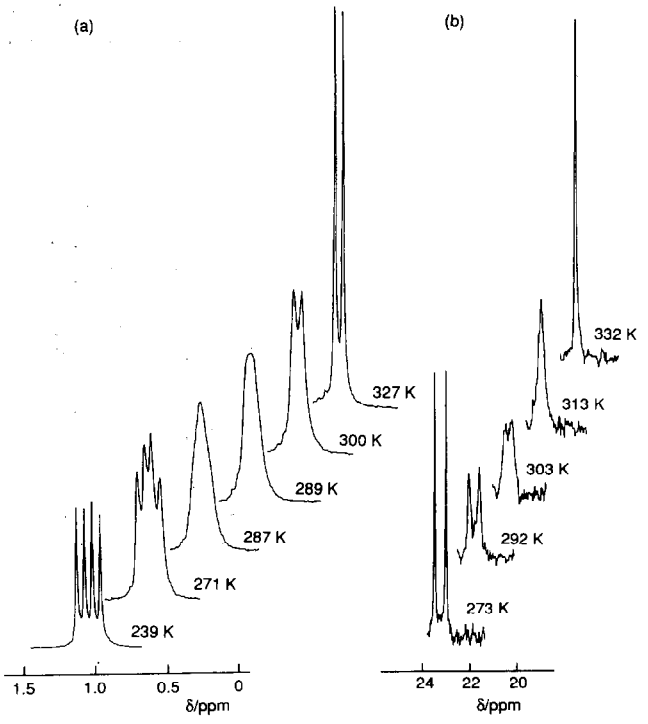

Fig. 2. Temperature-dependent NMR spectra of $Fe_2(CO)_8[\mu\text{-}Si\{O(2,6\text{-}^iPr_2C_6H_3)\}_2]$ (**2b**) (methyl region). (a) ^1H NMR spectra (90 MHz, CD_2Cl_2). (b) ^{13}C NMR spectra (22.5 MHz, CD_2Cl_2).

Complex **2b** shows fluxional behavior originating from the motion of the substituents on silicon. The temperature-dependent ^1H and ^{13}C NMR spectra of **2b** (methyl region) in CD_2Cl_2 are shown in Fig. 2. The ^1H NMR (90 MHz) signals of the methyl protons of isopropyl groups appear as two doublets at 239 K ($\Delta\nu$ = 13.2 Hz), but they coalesce as the temperature is raised and become only one doublet at 327 K. Similarly, the ^{13}C NMR spectrum (22.5 MHz) shows two methyl signals at 273 K ($\Delta\nu$ = 56.2 Hz), while only one at 332 K. During these changes, each of the methine protons and carbons of isopropyl groups was observed as one resonance, and kept unchanged. The mechanism for this dynamic NMR behavior is not clear in detail, but it is undoubtedly related to the hindered rotation of C(aromatic)–C(methine) or Si–O–C(aromatic) bonds. From the coalescence temperature (289 K) of the ^1H NMR spectrum, $\Delta G^{\ddagger}_{289\ K}$ of this process is estimated to be approximately 63 kJ mol^{-1}.

Acknowledgments

This work was supported by a Grant-in-Aid for Special Project Research No. 04241102 from the Ministry of Education, Science and Culture, and a Grant-in

Aid from the Nippon Sheet Glass Foundation for Material Science. We are grateful to Dow Corning Toray Silicone Co., Ltd. and Mitsubishi Materials Corporation for gifts of silicon compounds.

References

1 A.L. Bikovetz, O.V. Kuzmin, V.M. Vdovin and A.M. Krapivin, *J. Organomet. Chem., 194* (1980) C33.

2 M.J. Michalczyk, M.J. Fink, K.J. Haller, R. West, and J. Michl, *Organometallics, 5* (1986) 531.

3 M.J. Fink, M.J. Michalczyk, K.J. Haller, R. West, and J. Michl, *Organometallics, 3* (1984) 793.

4 R.B. King, *Organometallic Syntheses*, Vol. 1, Academic Press, New York, 1965, p. 93.

5 W. McFarlane and G. Wilkinson, *Inorg. Synth., 8* (1966) 181.

6 T. Sakurai and M. Kobayashi, *Rikagaku Kenkyusho Houkoku, 55* (1979) 69.

7 W.R. Dunnavant, R.A. Markle, P.B. Stickney, I.E. Curry and J.D. Byrd, Tech. Pap., Reg. Tech. Conf., Soc. Plast. Eng., Maiami Valley Sect., 1966, p. 19.

8 H. Weiss and H. Oehme, *Z. Anorg. Allg. Chem., 568* (1989) 157.

9 See, for instance: (a) R.K. Harris, J.D. Kennedy and W. McFarlane, in R.K. Harris and B.E. Mann (eds.), *NMR and the Periodic Table*, Academic Press, New York, 1978, pp. 309–377; (b) J. Schraml, in V. Chvalovsky and J.M. Bellama (eds.), *Carbon-Functional Organosilicon Compounds*, Plenum Press, New York, 1984, pp. 121–232.

10 Y. Kawano, H. Tobita and H. Ogino, *J. Organomet. Chem., 428* (1992) 125.

11 (a) H. Tobita, Y. Kawano and H. Ogino, *Chem. Lett.*, (1989) 2155; (b) K. Ueno, N. Hamashima, M. Shimoi and H. Ogino, *Organometallics, 10* (1991) 959; (c) Y. Kawano, H. Tobita and H. Ogino, *Organometallics, 11* (1992) 499.

12 S.G. Anema, G.C. Barris, K.M. Mackay and B.K. Nicholson, *J. Organomet. Chem., 350* (1988) 207.

13 For example, the Si–Fe distances of *cis*-$Fe(CO)_4(SiMe_3)_2$ and *cis*-$Fe(CO)_4(H)SiPh_3$ are 2.456(2) and 2.415(3) Å, respectively: L. Vancea, M.J. Bennett, C.E. Jones, R.A. Smith and W.A.G. Graham, *Inorg. Chem., 16* (1977) 897.